SOFT ROBOTICS
Volume 12, Number 1, 2025

DOI: 10.1089/soro.2023.0089

SoRo
Soft Robotics

ORIGINAL ARTICLE

Exo-Glove Shell: A Hybrid Rigid-Soft Wearable Robot for Thumb Opposition with an Under-Actuated Tendon-Driven System

Byungchul Kim,[1,2] Hyungmin Choi,[1] Kyubum Kim,[1] Sejin Jeong,[3] and Kyu-Jin Cho[1]

Abstract

Usability and functionality are important when designing hand-wearable robots; however, satisfying both indicators remains a challenging issue, even though researchers have made important progress with state-of-the-art robot components. Although hand-wearable robots require sufficient actuators and sensors considering their functionality, these components complicate the robot. Further, robot compliance should be carefully considered because it affects both indicators. For example, a robot's softness makes it compact (improving usability) but also induces inaccurate force transmission (impacting functionality). To address this issue, we present in this paper a tendon-driven, hybrid, hand-wearable robot, named Exo-Glove Shell. The proposed robot assists in three primitive motions (i.e., thumb opposition motion, which is known as one of the most important hand functions, and flexion/extension of the index/middle fingers) while employing only four actuators by using an under-actuation mechanism. The Exo-Glove Shell was designed by combining a soft robotic body with rigid tendon router modules. The use of soft garments enables the robot to be fitted well to users without customization or adjustment of the mechanisms; the metal routers facilitate accurate force transmission. User tests conducted with an individual with a spinal cord injury (SCI) found that the robot could sufficiently and reliably assist in three primitive motions through its four actuators. The research also determined that the robot can assist in various postures with sufficient stability. Based on the grasp stability index proposed in this paper, user stability—when assisted by the proposed robot—was found to be 4.75 times that of an SCI person who did not use the Exo-Glove Shell.

Keywords: soft tendon-driven wearable robot, under-actuated mechanism, hybrid soft-rigid wearable robot

[1]Biorobotics Laboratory, Department of Mechanical Engineering/Soft Robotics Research Center (SRRC)/Institute of Advanced Machines and Design (IAMD)/Institute of Engineering Research, Seoul National University, Seoul, Korea.
[2]Distributed Robotics Laboratory, Computer Science and Artificial Intelligence Laboratory (CSAIL), Massachusetts Institute of Technology, Cambridge, Massachusetts, USA.
[3]Institute of Art, Department of Design and Craft, Seoul National University, Seoul, Korea.
This work was done at SNU.

Introduction

The human hand has crucial roles in activities of daily living (ADL), relying on its ability to generate high DOF motions. Unfortunately, individuals who have lost hand function owing to spinal cord injury (SCI),[1] cerebral palsy,[2] or stroke[3] face significant limitations when engaging in ADL. To address it, researchers have shown keen interest in hand-wearable robots, recognizing their potential to enhance the quality of life.[4–13]

Researchers investigating hand-wearable robots have prioritized minimizing size and weight, acknowledging the need for user comfort while wearing the robot.[14] To achieve compactness, lightweightness, and portability, some researchers have developed wearable robots using soft material, called soft wearable robots (SWRs), which can easily adapt to the user's body without extra mechanisms.[15–25] They have also incorporated tendon transmission in their robots to fully leverage its benefits, simplifying the robot end-effector (See Supplementary Appendix S1 for other transmissions used in SWRs).[26,27] Although these approaches have reduced the complexity and weight of the robot, developing tendon-driven soft wearable robots (T-SWRs) capable of accommodating versatile hand functions has presented challenges.

They sometimes generate inaccurate postures when the tendon causes unwanted deformation of the robot body (Supplementary Video S1)—that is, the tendon deforms the robot body (e.g., when extending the finger (Fig. 1b) if deforming the robot requires less energy than that when extending the finger; the unwanted deformation is not preferred because it induces inaccurate posture by reducing the tendon moment arm. As the robot body is made of soft material, preventing unwanted deformation during actuation has proven to be challenging.[28,29]

The difficulties of the robot fabrication process are other issues that make robot development challenging. Fabric-based robots require manual sewing, which demands delicate hand skills, whereas silicone-based robots involve time-consuming manual molding. Moreover, these fabrication methods are irreversible, making it difficult to modify the robot after production. To simplify fabrication, some researchers have turned to 3D printers for building robots.[5,30–33] However, despite alleviating fabrication difficulties, reducing the thickness of the robot remains challenging with this method, because 3D-printed parts tend to be weaker compared to fabric-based structures when thin. Considering the narrow space between fingers, the thickness is a crucial factor in ensuring usability.

Another challenge in developing T-SWRs pertains to the number of required actuators.[34–37] As tendons only transmit tensile force, the robot necessitates two actuators for each joint.[14] Although there exist smart methods to reduce the number of actuators, they require researchers to carefully consider the physical properties (such as joint stiffness or finger size) of the users before fabricating the robot (Supplementary Appendix S1).[35,37]

In light of existing challenges, we have developed a T-SWR considering the following issues:

1. Prevention of unwanted robot body deformation, particularly at the points where tension is applied, to ensure accurate hand-posture assistance.
2. Fabricating a reliable yet low-profile structure with minimal fabrication difficulties to expedite the design iteration.
3. Exploration of methods to minimize the number of actuators, as the tendon can only transmit tensile force.

In this paper, to address the above considerations, we propose Exo-Glove Shell, a T-SWR developed to assist

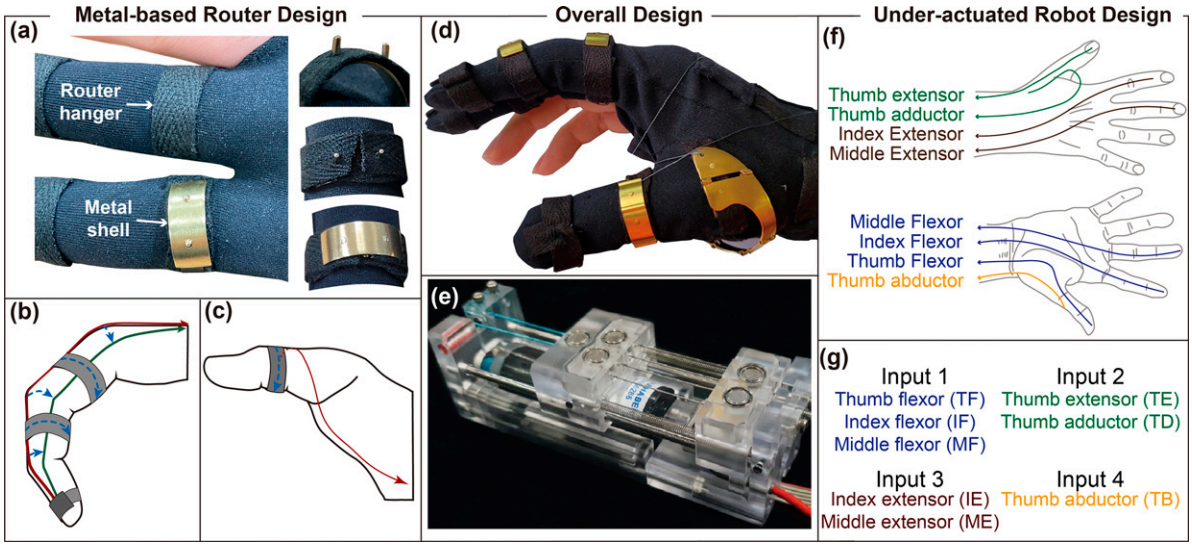

FIG. 1. Two main design features of the Exo-Glove Shell: hybrid rigid-soft wearable robot design **(a–d)** and under-actuated tendon routing for three primitive motions with four actuators **(e–g).** **(a)** shows how the metal router is attached to the robot using router hanger; **(b)** and **(c)** show possible problems that can occur when the robot is not fixed well to the user body; **(d)** shows the Exo-Glove Shell fabricated with both a soft garment and metal router; **(e)** shows the specifically designed actuator for the under-actuation mechanism without complicating the robot end-effector; **(f)** and **(g)** shows how the tendons are routed along the glove to enable the desired motions with less actuators.

individuals with SCI to perform ADL. The robot (Fig. 1) consists of a soft garment that enables a simple wearing part and metal ring structures that allow for accurate force transmission. The inclusion of metal rings dramatically reduces difficulties in fabrication as they can be attached after the glove is fabricated. Further, by incorporating an under-actuation mechanism between the fingers, the proposed robot operates with the minimum number of actuators required to assist essential grasp motions encountered in daily life. The following are the detailed design methods and research contributions:

1. *Hybrid design with a soft glove and metal routers for functional decoupling*

   Our soft robotic glove ensures easy wearing and a comfortable fit for the user. Composing the routers, which fix the tendon path, with a metal structure enables to route of the tendon firmly, enabling accurate force transmission. As these metal routers are strong enough even with the thin structure, developing the robot to have a thin profile is also possible.

2. *Three-step fabrication for ease of manufacturing and enabling design changes*

   The glove used in our robot can be easily manufactured owing to their design similarity to general-use gloves made for nondisabled individuals. This is because tendon routers can be attached after the glove's fabrication. Further, the riveting used to attach the metal routers to the glove is an easier method as compared with other bonding methods (e.g., sewing or silicone adhesion) used in other SWR fabrication. The decoupled functions of the two robot components also facilitate design modifications, such as changing the tendon routing by simply detaching the original metal router and attaching the other metal router with a different structure. Previously, because modifying the design after fabrication was difficult when the robots were made by sewing or molding, any change required the fabrication of new robot.

3. *Assistance with three primitive motions with only four actuators*

   To reduce the number of actuators, we extended the use of the under-actuation mechanism to use it between the fingers; in contrast, most SWRs use it inside the finger. This approach enables the robot to assist in three primitive motions (thumb opposition and index/middle finger flexion/extension) with four actuators. The motions to be assisted were chosen according to biomechanic studies demonstrating the importance of thumb opposition.[38] The actuator count was derived through simulation (Section 4.1) and confirmed by experimental validation.

Design

The proposed robot's wearing part is designed with two essential components: the "robot body" and the "tendon router." This is because they have significant impacts on the robot's performance, yet they have contrasting requirements. To address these requirements, we fabricated the robot body as a fabric-based soft glove, ensuring a lightweight, compact, and easy-to-wear wearing part. In contrast, the tendon router was developed as a metal router, securely fixing the tendon path to enhance actuation reliability. The fabrication process involved separately producing the robot body and tendon router, followed by their combination. This functional decouple and three-step fabrication method offers the following advantages: 1) easy wearing and improved actuation reliability; 2) reduced difficulties in the robot fabrication; and 3) modular design (design approach that enables researchers to design the part differently for each body part, considering the different requirements of each setting) of the tendon router.

Design of fabric-based glove

The robot body is designed with the following considerations: it should 1) be easily wearable for individuals with disabilities; 2) have a compact size and be lightweight; and 3) fix the tendon router without occupying a large conjunction volume. For easy wearing, the robot body is fabricated in a glove form using a thin, stretchable, and low-friction fabric. It is important to note that our novel design approach, which incorporates metal routers to complement the actuation stability, enables us to use such fabric. Without reliable routers, the use of such fabric could result in unsteady movement caused by deformation in robot bodies (Supplementary Video S1). The robot body has a unique component called *router hanger* (Fig. 2c and Supplementary Appendix S2). It is made of a herringbone tape and is sewn at the glove to enable compact and easy attachment of the tendon routers.

Design of metal-based shell router

In contrast to the design requirements for the fabric-based glove, we focused on the reliable actuation and modular design when designing the tendon router. For improved actuation reliability, routers are made of metal to prevent unwanted robot deformation that could lead to inaccurate force transmission (See Fig. 1b, c and Supplementary Video S1). For compact conjunction and modular design, the router was designed to consist of two components, a *router base* and a *router cover* (Fig. 2a and b), to attach the router to the glove through riveting.

The attachment process involved placing the router base under the router hanger (Fig. 2d-1), with two horns of the base piercing the router hanger. Next, the *router cover* was positioned on the two horns of the base that protruded through the router hanger (Fig. 2d-2). Finally, the routers were fixed to the glove by riveting the horns (Fig. 2d-3).

Riveting allowed for modularization of the tendon router design because we could attach the tendon router to the glove as long as there are two holes in the router cover. Consequently, the router covers can be developed differently depending on their intended attachment locations as shown in Figure 2b. This feature expanded our opportunities to satisfy varying requirements based on their installation positions.

Routers for the index/middle finger were designed to avoid interference with other routers, considering the narrow space between the fingers. The thumb MCP router was developed to ensure a firm fixation, employing a ring-type

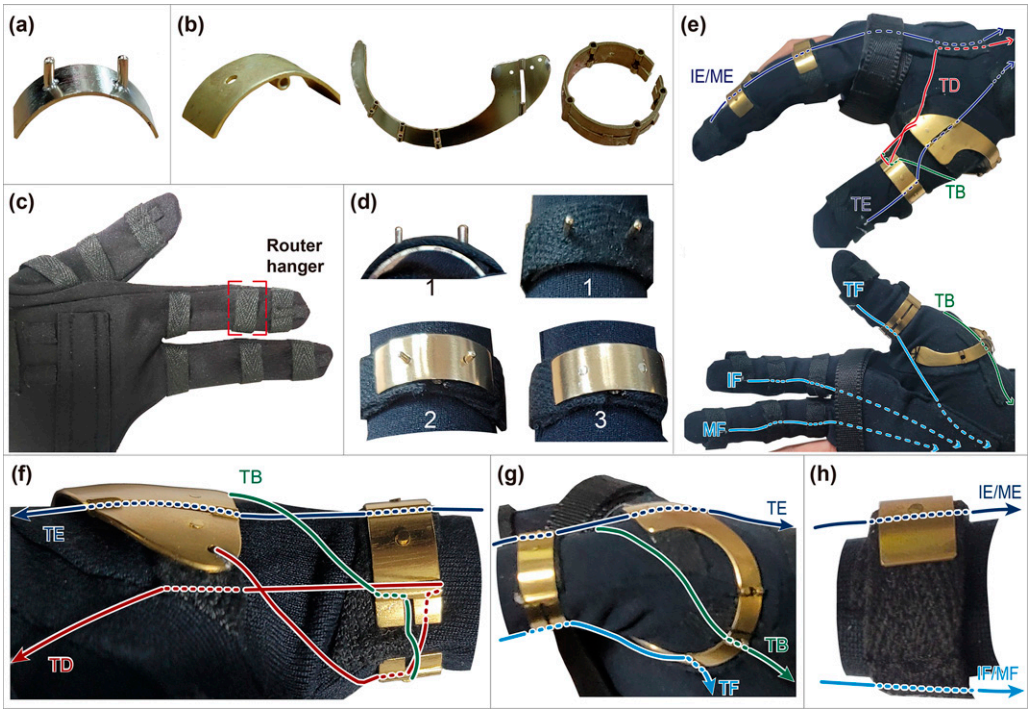

FIG. 2. Design of the glove and tendon routers. **(a)** shows the shell base of the tendon router and **(b)** shows the shell cover of the router. From the left, the figure shows the shell cover of the index/middle tendon router, thumb CMC joint router, and thumb MCP joint router. **(c)** shows the robot basement in the shape of a glove; **(d)** shows the overall process of attaching the metal router to the glove (a more detailed explanation is in Appendix); **(e)** shows the overall tendon routing of the Exo-Glove Shell, where IE/ME, TD, TE, and TB represent index extensor/middle extensor, thumb adductor, thumb extensor, and thumb abductor, respectively; IF, MF, TF, and TB represent index flexor, middle flexor, thumb flexor, and thumb abductor, respectively. **(f)** and **(g)** show a magnified picture that describes the tendon routing of the thumb routers, whereas **(h)** shows the tendon routing of the index/middle router.

metal structure. The thumb CMC router was designed to be deformable for a better fit with various hand shapes. Further details are provided in Supplementary Appendix S2.

Under-actuated tendon routing

Previous research that examined pulley-based tendon transmissions has shown that $n + 1$ number of actuators can make n-DOF motions.[26] Accordingly, it is reasonable to use four actuators for the Exo-Glove Shell because it is designed to assist three primitive motions. However, the Exo-Glove Shell uses suspended tendon transmission rather than pulley-based transmission owing to the compactness, raising the possibility that four actuators may not be sufficient (Supplementary Appendix S3). To determine the adequacy of using four actuators in our case, we conducted both simulations (Subsection 4.1) and experiments (Subsection 4.3).

Based on the simulation result (Section 4.1), which showed that four actuators are sufficient, we developed the Exo-Glove Shell with an under-actuation mechanism between the fingers. It is worth noting that despite the use of under-actuation, the wearing part of the robot remains simple because specific actuators designed for under-actuated tendon routing were utilized for robot development.[39] The actuators pull eight tendons (Fig. 1g) as follows: *Actuator1*—thumb, index, and middle finger flexors; *Actuator2*—a thumb abductor; *Actuator3*—index and middle finger extensors; and *Actuator4*—a thumb extensor and an adductor. Among several possibilities to configure tendons, we used this configuration owing to several reasons. The under-actuation mechanism is applied in the flexion of three fingers to make an adaptive grasp. For the thumb abduction, we decided to pull the abductor with a single actuator due to its crucial role in forming the hand's posture before grasping. The extensor of the index and middle fingers was designed to be pulled by a single actuator based on satisfactory performance observed in our previous research.[28,37] The remaining tendons for the thumb adduction and the thumb extension were also designed to be pulled by an actuator via an under-actuation mechanism.

Method

Target motion definition

Following the previous research,[40,41] we divided the grasping process into the pre-grasp phase and the actual grasp phase. This paper specifically focuses on two diffe-rent grasp postures, namely the power grasp and the lateral pinch grasp.

During the pre-grasp phase of power grasp assistance, our objective was to position the thumb on the opposite side of the other fingers. To achieve this, we took the index finger plane (represented by a dotted line in Fig. 3a) as a reference. The pre-grasp for the power grasp was designed to meet the following conditions:

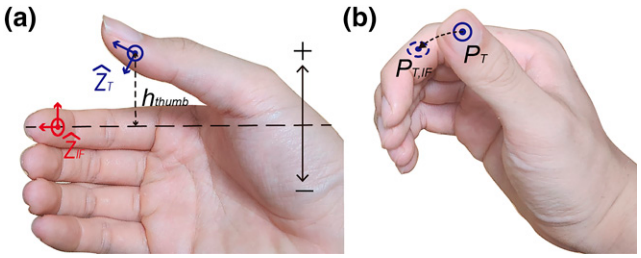

FIG. 3. Variables to represent targeted hand postures in the pre-grasp phase. **(a)** shows variables to describe the targeted hand posture in the pre-grasp phase of the power grasp. Here, the $\hat{Z}$ of each coordinate is parallel to the normal vector from the finger skin. The dotted line at the center of the index finger represents the index finger plane. **(b)** shows the variables used to describe the targeted hand posture in the pre-grasp phase of the lateral pinch grasp. The tip of Thumb (P_T) should be located where it can press the side of index finger ($P_{T,IF}$) at the actual grasp stage.

$$\begin{aligned} & h_{thumb} \leq 0 \\ & min(C_{thumb}) = min(\angle(\hat{Z}_{IF}, \hat{Z}_T)) \end{aligned} \tag{1}$$

where $\hat{Z}_{IF}$ and $\hat{Z}_T$ are the z-axis of the index finger and the thumb represented in the global frame, respectively; h_{thumb} is the height of the thumb defined in the index coordinate (i.e., the distance between the thumb and index finger plane); C_{thumb} is the angle between thumb normal vector and the index finger normal vector. We wanted to minimize C_{thumb} because it makes more stable grasp, as explained in the Supplementary Appendix S1. These variables are visualized in Figure 3a.

The robot locates the thumb in a position such that the thumb height ($\hat{Z}_T$) is below zero at the pre-grasp phase to guarantee stability in the actual grasp phase. Specifically, when the thumb height is zero, the thumb faces the index finger, whereas a negative height causes it to face the other fingers. We can also infer that minimizing the angle between two vectors ($\hat{Z}_{IF}$ and $\hat{Z}_T$ in Eq. (1) improves the grasp stability.

In the lateral pinch assistance, our objective during the pre-grasp stage was to pre-position the thumb in such a way that it could exert force on the side of the index finger during the actual grasp phase. Specifically, we aimed for the estimated thumb position in the actual grasp phase, denoted as $P_{T,IF}$ (as depicted in Fig. 3b), to be located within the workspace of the index finger. Therefore, in the pre-grasp phase, we wanted the robot to locate the user thumb at P_T (as shown in Fig. 3b). Details on desired thumb location in lateral pinch grasp (including the relationship between thumb position at pre-grasp and actual grasp phase) are elaborated in Supplementary Appendix S4.

Experimental design

We designed four experiments to prove our hypothesis about metal routers and under-actuated tendon routing. The metal router experiment involved one healthy subject, whereas the other experiments were performed with an SCI subject who does not have hand mobility (See Supplementary Appendix S4 for detailed experimental protocols). All procedures were approved by the Institutional Review Board of Seoul National University (IRB No. 22014/001-004).

The first experiment is designed to show the anchoring ability of the metal router; it measures how much the router tilts against the finger when repeating the flexion/extension of the index finger. To see the benefits of using metal routers, the tilted angle of the router of both the proposed robot (Exo-Glove Shell) and the previous robot (Exo-Glove) was measured.

We conducted the second experiment to show whether the Exo-Glove Shell can assist three primitive motions, using indicators that represent three primitive motions. The indicators were defined as

$$\begin{aligned} Q_{TABD} &= q_{CMC.ABD} \\ Q_{TFE} &= mean(q_{CMC.FE}, q_{MCP.FE}, q_{IP.FE}) \\ Q_{MIFE} &= mean(q_{I.FE}, q_{M.FE}) \end{aligned} \tag{2}$$

where, $q_{joint,direction}$ is the joint angle in a specific direction.

For the third experiment, we aimed to evaluate the effectiveness of our robot in assisting ADL by focusing on power grasp and lateral pinch grasp explained in Subsection 3.1. To prove whether Exo-Glove Shell assists power grasp properly, we measured how the thumb height and the orientation angle (defined in Eq. (1)) vary when the robot assists the pre-grasp. For the lateral pinch grasp assistance performance, an experiment is conducted to simultaneously measure the index finger workspace and the thumb location to obtain $P_{T,IF}$ and P_T defined in Figure 3. Both experiments about power grasp and lateral pinch grasp measure the joint angle indicators defined in Eq. (2) to show how our robot assists the user during the entire grasping process.

The last experiment validates whether the robot can assist the user in making a firm grasp. To measure the grasping force, we designed a custom experimental setup (Fig. 4) that measures the sum of the contact force applied to the object, deviating from other methods used in previous studies.[28,37] The rationale behind employing the new setup is elaborated in Supplementary Appendix S4.

Using this experimental setup, we measured the grasp performance factor (P_{force}) in the force domain, which is defined as

$$\begin{aligned} P_{force} &= \sum_{i=1}^{n} F_{c,i} \\ &\simeq F_L / \mu_k \end{aligned} \tag{3}$$

where $F_{c,i}$ is a contact force applied at the contact point i, F_L is the force measured at the loadcell, and μ_k is a friction coefficient between the robot and the object.

Results

Simulation 1—Simulation to determine a proper number of actuators for the Exo-Glove Shell

Unlike previous studies,[26] we cannot analytically derive the required number of actuators to make n DOF motions in the case of the Exo-Glove Shell. This difference occurs

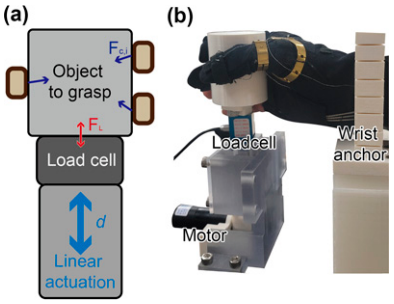

FIG. 4. Experimental setup used to validate the grasping force. **(a)** shows a schematic of the grasping force measurement setup; **(b)** shows how the real experiment was conducted using the proposed robot.

because our robot has a suspended tendon routed system that induces a nonlinear relationship between the joint angle and the actuation input.[26,29] Therefore, we investigated the robot's performance according to the number of actuators through simulation. The simulation was conducted with an objective function as a volume of the *opposition workspace*.[42] This is because the main objective of the Exo-Glove Shell is to assist the opposition motion.

Using the simulation process (Supplementary Appendix S3), the opposition workspace planes for different numbers of actuators (ranging from one to six) were compared with the workspace of the case that uses six actuators (Fig. 5). We also calculated the area of each of the opposition workspace results, as shown in Table 1. According to the ratio described in this table, we observed a significant increase in the volume of the workspace as the number of actuators increased from three to four. As the performance of the robot that uses four actuators reached 96% of that of the robot when using six actuators, we concluded that using four actuators is reasonable for the development of the Exo-Glove Shell.

Experiment 1—Experiment to measure router performance

We measured the tilted angle of the router (θ_{tilt}) for 50 times (25 for each robot) (Fig. 6). The averages of θ_{tilt} were 0.257 (rad) and 0.074 (rad) when Exo-Glove and Exo-Glove Shell were used, respectively, whereas the variances were 0.016 (rad) and 0.066 (rad), respectively. The smaller average and variance of θ_{tilt} indicate a small shift of the router, suggesting that the Exo-Glove Shell has better reliability in robot operation compared to the previous design. The impact of the router's anchoring ability on the actual robot performance can be observed in the Supplementary Video S1.

Experiment 2—Experimental analysis of three primitive motions

In this experiment, we measured joint angle indicators (defined in Eq. 2) when assisting the thumb abduction/adduction motion (Fig. 7a and d), the thumb flexion/extension motion (Fig. 7b and e), and the flexion/extension motion of the middle/index fingers (Fig. 7c and f).

The results show that the Exo-Glove Shell can independently assist fingers in three directions with four actuators,

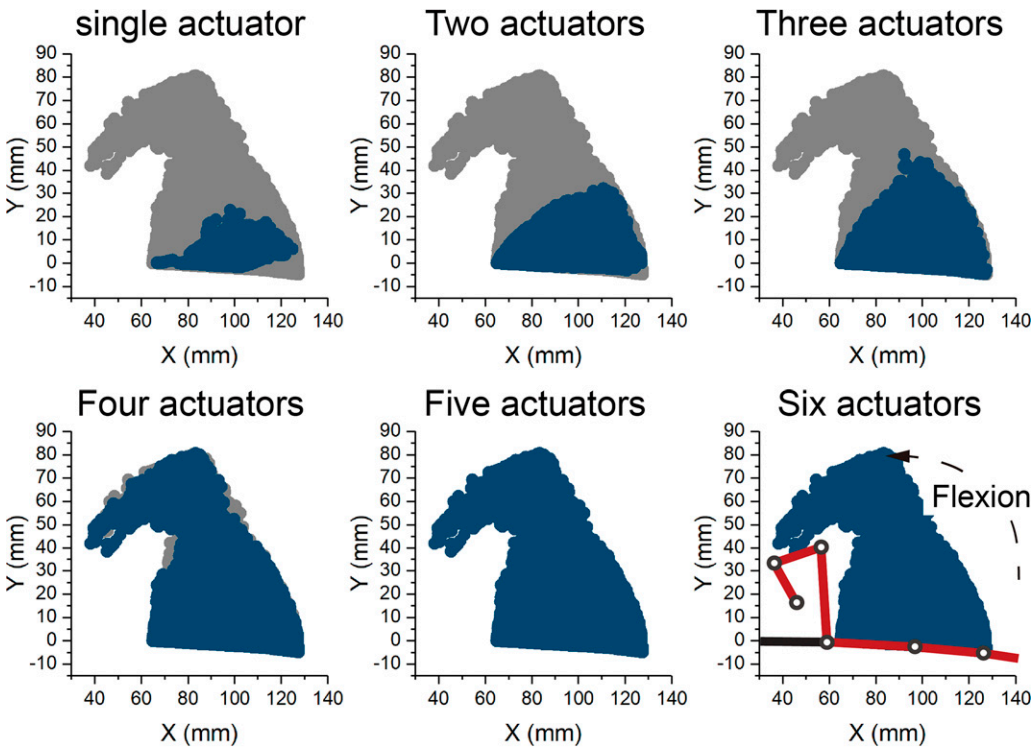

FIG. 5. Opposition workspace according to the number of actuators. The gray area in the figure shows the opposition workspace (Space where the thumb's workspace and the index/middle fingers' workspace overlap) when six actuators are used, and the blue area shows the opposition workspace when each specific number of actuators was used. The red lines in the six-actuator case describe the estimated flexion/extension motion of the index/middle finger.

Table 1. Opposition Workspace Size According to the Number of Actuators

	Number of actuators					
	1	*2*	*3*	*4*	*5*	*6*
Area (mm^2)	699.5	1355.2	1812.1	3862.2	3975.8	4004.2
Ratio	0.175	0.338	0.453	0.956	0.993	1

confirming our findings from the simulation results. The upper figures show the angle indicators in the time domain conducted five times. The lower figures describe the average and variance of the angle indicators obtained at each trial. Although there is a small amount of coupled motion, it is negligible in practice (Supplementary Video S1 and Supplementary Appendix S3).

Experiment 3—Experiment that verifies the grasp assistance of the Exo-Glove Shell

The results (Fig. 8a) indicate that the thumb height (h_{thumb}), represented in the index coordinate system, becomes negative as the thumb abductor pulls the thumb. This signifies that the proposed robot effectively assists the pre-grasp phase of the power grasp by positioning the thumb to face the other fingers. The thumb abduction also reduces the thumb orientation angle, C_{thumb} (Fig. 8a). From the relationship between the thumb height and the orientation angle (Fig. 8b), we can infer that the robot decreases the orientation angle between the thumb and the other fingers during the pre-grasp phase. This decreased angle makes a more stable grasp during the actual grasp phase.

The entire grasping process of the power grasp assistance can be found in Figure 8c with joint angle indicators defined in Eq (2). Our robot assists the pre-grasp at time T_0 by abducting the thumb. After making the pre-grasp posture, the robot initiates the actual grasp assistance at time T_1, involving the flexion of three fingers. Subsequently, the robot finishes the grasp assistance by extending all fingers at time T_2 to complete the grasping process.

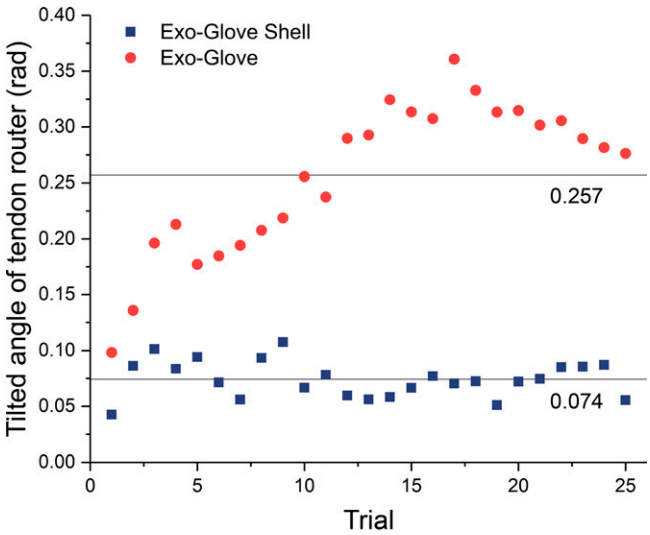

FIG. 6. Experimental results that show the performance of the metal routers. Results of Experiment 1 that show how much the router shifts when the robots (Exo-Glove Shell and Exo-Glove) operate repeatedly. The straight lines mean the average values of the tilted angle of the Exo-Glove and Exo-Glove Shell. A larger average means the router is more unstable because it is tilted more away from the user's body. Please see the Supplementary Video to see why a tilted angle harms the stability.

For the lateral pinch grasp assistance, we measured the thumb location (P_T and $P_{T,IF}$ defined in Subsection 3.2) as shown in Figure 9a. It shows that the Exo-Glove Shell effectively locates the thumb in a position where it can exert force on the side of the index finger. Similar to the power grasp experiment, the joint angle indicators are obtained (Fig. 9b). The result shows entire lateral grasp assistance as follows: initially, at time T_0, the robot assists thumb adduction and extension to position the thumb appropriately within the index finger's workspace. It is worth noting that due to under-actuated tendon routing of the Exo-Glove Shell, it can be simply done by pulling a single actuator (Input 2 in Fig. 1g). Subsequently, at time T_1, the robot flexed the index and middle fingers so that the orthographic projection of the thumb ($P_{T,IF}$) toward the index plane can cross the index finger. At the time T_2, the robot further assisted thumb flexion, thereby enabling the actual grasp. Finally, the robot concluded the grasp assistance by extending the thumb at time T_3.

We also have obtained the detailed duration time for two different grasp assistances (Table 2). In addition, to validate the practical applicability of the Exo-Glove Shell for individuals with spinal cord injuries, we conducted an experiment involving the grasping of various objects as depicted in (Fig. 10).

Experiment 4—Experiment to measure grasping force

The grasp performance (P_{force}) was assessed by comparing the measurements obtained when the user was assisted by the Exo-Glove Shell with those measured when the user did not utilize the robot. To examine the influence of different grasp postures on performance, we conducted experiments using both a cylinder-shaped object (that is grasped by power grasp) and a card-shaped object (that is grasped by lateral pinch). The results are presented in Table 3, indicating that the grasp stability achieved with the assistance of the robot was 4.75 times greater than that of an individual with SCI who did not use the robot.

Discussion & Conclusion

This paper proposes the Exo-Glove Shell, a novel tendon-driven hybrid soft-rigid wearable robot with a focus on balancing functionality and usability. The research introduces two key contributions: 1) the integration of a soft-garment-based wearing part with rigid-metal-based tendon routers and 2) the incorporation of an under-actuation mechanism

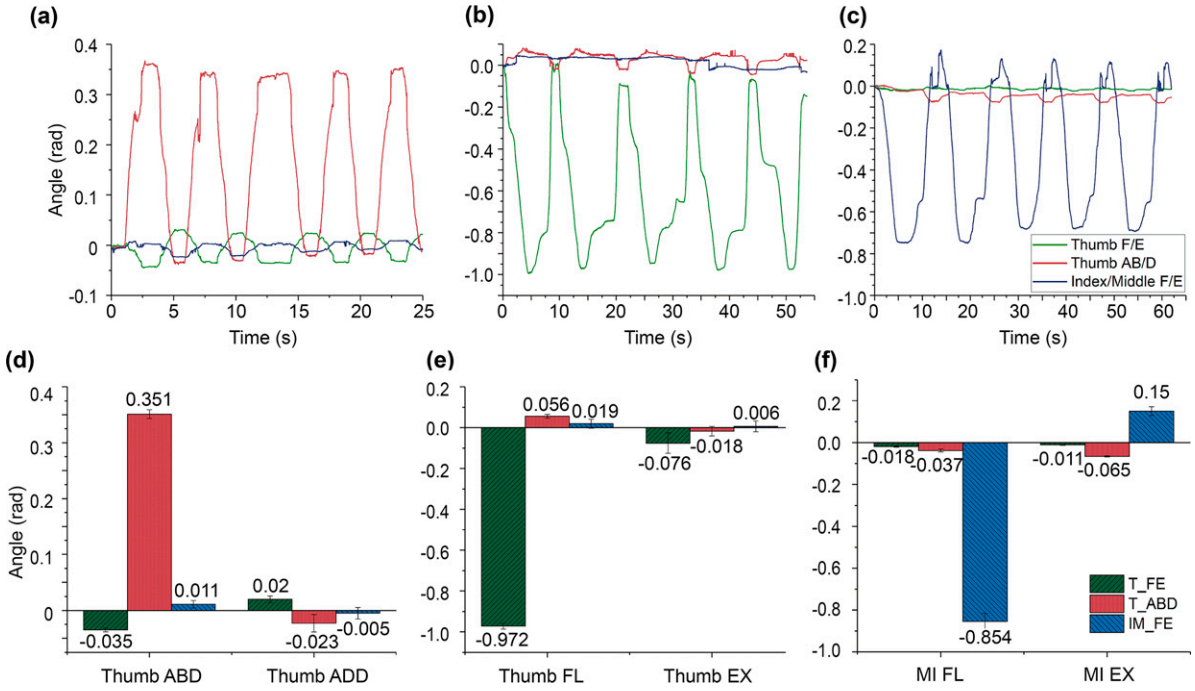

FIG. 7. Experiment results that show that the proposed robot can assist in three primitive motions independently. **(a)** and **(d)** show how the fingers move when assisting the thumb abduction/adduction motion; **(b)** and **(e)** show the joint motions for the thumb flexion/extension motion; **(c)** and **(f)** show the joint motions of the flexion/extension motion of the middle/index finger. The graph legend in **(c)** is for **(a)–(c)** and the legend in **(f)** is for **(d)–(f)**; F/E and AB/D indicate flexion/extension and abduction/adduction; FL and EX indicate flexion and extension; ABD and ADD mean abduction and adduction. In this analysis, flexion and adduction were expressed as angles with negative values, and extension and adduction were expressed as angles with positive values.

to find an ideal number of actuators for desired primitive motions.

Recent studies have used materials with different stiffness to augment the capabilities of SWRs.[4,43,44] Building on top of these approaches, our research demonstrates the efficacy of a hybrid rigid-SWR design framework in enhancing the reliability of force transmission. The contribution of this paper lies not only in the integration of metal structures into wearable robots for reliable force transmission but also in the systematic categorization of robotic functions and the development of specialized design and fabrication techniques tailored to each function.

We contend that our findings provide a foundation for other researchers to create wearable robots for diverse body parts utilizing standard clothing patterns available online. This approach reduces the need for extensive expertise in wearable robot fabrication. A pivotal aspect of this process is the incorporation of *soft hangers*. Subsequently, the researchers can develop their own wearable robots by attaching *modularized rigid routers*, components that are

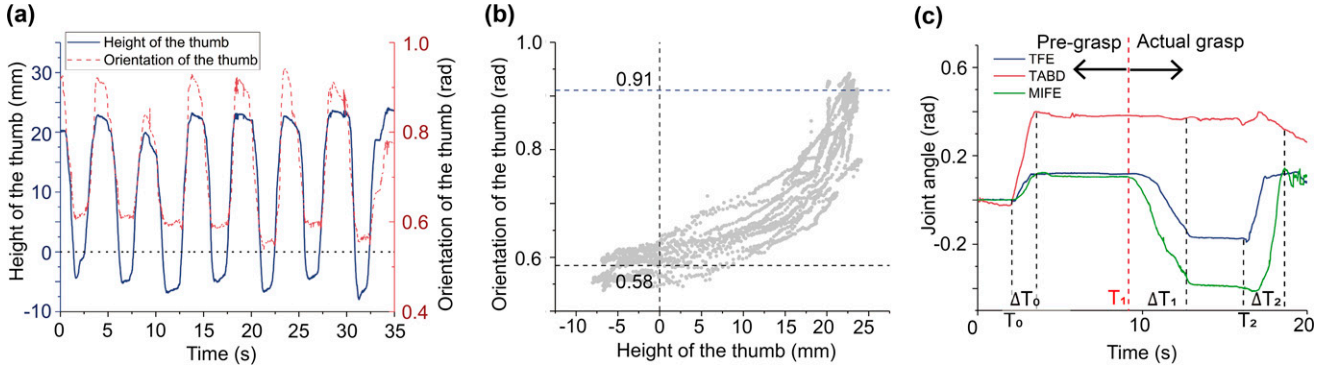

FIG. 8. Experimental results that show how the proposed robot assists with a power grasp. **(a)** shows how the proposed robot positions the thumb during the pre-grasp phase when assisting the power grasp; it shows that the thumb height reduces from a positive value to a negative value to be aligned to the other fingers. **(b)** shows how the thumb direction changes depending on the thumb position; the reduced orientation means that the thumb is more facing to the other fingers. **(c)** shows how three joint angle indicators defined in Eq (2) change when assisting the power grasp with the proposed robot. ΔT s in the graph represent the duration time of each stage; the exact values can be seen in Table 2. The height (h_{thumb}) and orientation (C_{thumb}) of the thumb in this figure are defined in Eq (2).

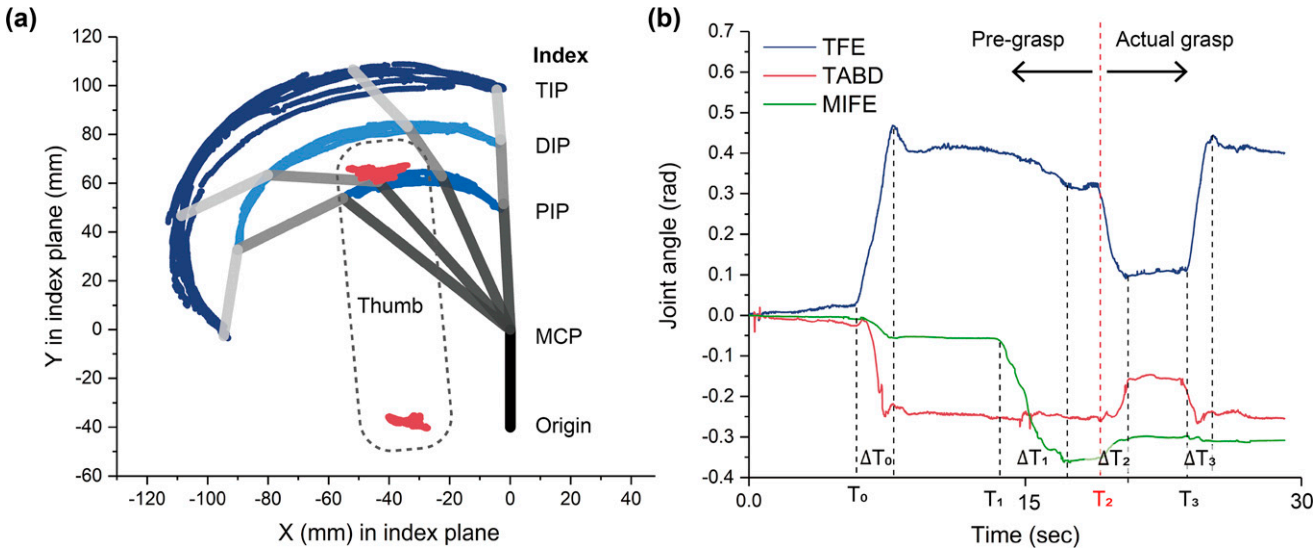

FIG. 9. Experimental results that show how the proposed robot assists with a lateral pinch grasp. **(a)** shows how the proposed robot positions the thumb, index, and middle finger during the pre-grasp phase when assisting with a lateral pinch grasp. Here, the red areas at the upper side show the location of the tip of the thumb and the red areas at the lower side show the CMC joint of the thumb; blue lines show the trajectory of the tip, DIP joint, and PIP joint of the index finger; the dotted line shows the estimated appearance of the thumb. **(b)** shows how three joint angle indicators defined in Eq (2) change when assisting the lateral pinch grasp with the proposed robot. ΔT s in the graph represent the duration time of each stage; the exact values can be seen in Table 2.

customized according to the specific characteristics of the body part they are designed for, to the *soft hanger*; our qualitative result (Supplementary Appendix S4) also shows the efficacy of metal routers, which are designed considering the thumb biomechanics, in assisting the thumb.

Addressing the question, "How many actuators are optimal in hand-wearable robots?" has emerged as a compelling research topic for hand-wearable robot researchers. In pursuit of using the least number of actuators necessary, some researchers have adopted the concept of *postural synergy* or *under-actuation mechanisms*. Conversely, others, focusing on developing a robot that can assist dexterous hand movements, have used actuators without specific limitations on their count. Distinct from these approaches, our study seeks to determine an ideal number of actuators that achieve a balance between usability and functionality. For this approach, we first determined to assist three primary motions based on hand biomechanics research: thumb abduction/adduction, thumb flexion/extension, and index/middle finger flexion/extension. Subsequently, through both simulation (Fig. 5) and experimental results (Fig. 7), we have identified the ideal number of actuators necessary to independently enable these motions; from these results, the Exo-Glove Shell is developed with four actuators.

Overall, the Exo-Glove Shell demonstrated the capability to assist various postures with adequate grasping force. The proposed grasping force performance index showed that a disabled individual experienced an average increase of 4.75 times in grasping ability when using the Exo-Glove Shell compared to unassisted grasping.

Our study's limitations include the absence of sensors on the wearable part, leading to heuristic control of the user's posture. Future work will integrate cameras for better joint angle estimation and intention detection, enhancing performance and usability. Although our robot, with a low-level controller using empirically found desired position/force, has assisted various motions with four actuators, the experiments were limited to a single SCI subject such as other pilot study papers.[5,12,45–48] To

TABLE 2. DURATION OF TIME WHEN ASSISTING POWER GRASP AND LATERAL PINCH GRASP

Power grasp		*Lateral pinch grasp*	
Grasp stage	*Duration*	*Grasp stage*	*Duration*
Pre-grasp (thumb abduction) (ΔT_0 in Fig. 8c)	1.56 (s)	Pre-grasp 1 (thumb adduction) (ΔT_0 in Fig. 9b)	2.04 (s)
—	—	Pre-grasp 2 (index/middle finger flexion) (ΔT_1 in Fig. 9b)	3.69 (s)
Actual grasp (index/middle finger flexion) (ΔT_1 in Fig. 8c)	3.66 (s)	Actual grasp (thumb flexion) (ΔT_2 in Fig. 9b)	1.52 (s)
Release (index/middle finger extension) (ΔT_2 in Fig. 8c)	2.61 (s)	Release (index/middle finger extension) (ΔT_3 in Fig. 9b)	1.37 (s)

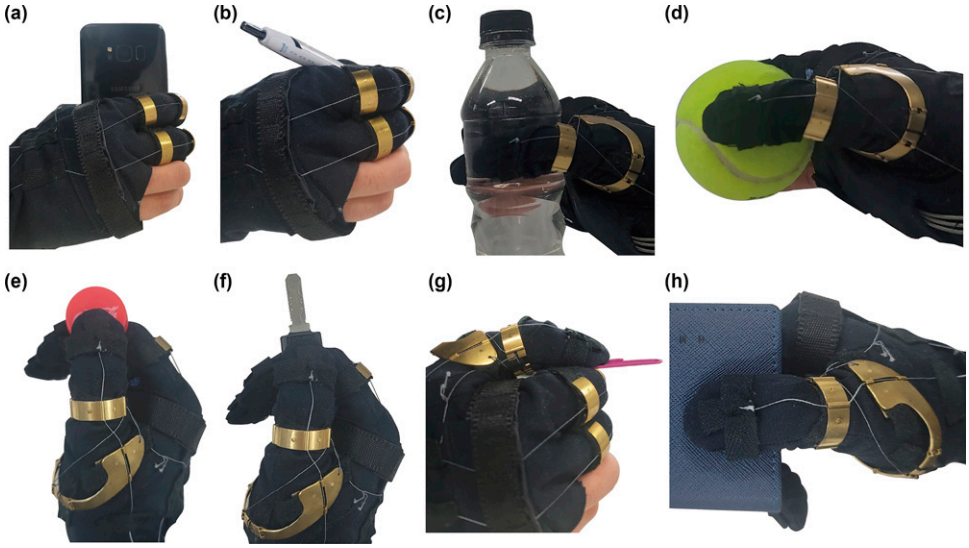

FIG. 10. Photographs of grasping various objects with the Exo-Glove Shell. **(a)–(d)** show the power grasp assistance of the Exo-Glove Shell and **(e)–(h)** show the lateral pinch grasp assistance of the Exo-Glove Shell. Each figure represents **(a)** grasping a phone; **(b)** grasping a pen; **(c)** grasping a bottle; **(d)** grasping a ball; **(e)** grasping a lid; **(f)** grasping a key; **(g)** grasping a clip; and **(h)** grasping a card wallet.

ensure broader applicability and robustness, future studies will conduct experiments with more subjects after developing a new version of the robot with a high-level controller adaptable to different human physical characteristics.

We hope that this research will provide the practical application of wearable robots beyond laboratory settings. We believe this research makes an important step in that direction because the proposed design methodologies have successfully solved the trade-off issue between the robot's usability and functionality.

Author Disclosure Statement

The authors do not have interests to disclose.

Funding Information

This research was supported by a National Research Foundation of Korea (NRF) Grant funded by the Korean Government (MSIT) under Project Number RS-2023-00208052 and a grant of the Korea Health Technology R&D Project through the Korea Health Industry Development Institute (KHIDI), funded by the Ministry of Health & Welfare, Republic of Korea (grant number: HI19C1352).

Table 3. Experimental Results that Show the Grasping Force Results

	Person with SCI	
	With Exo-Glove Shell	*Without Exo-Glove Shell*
Power Grasp	15.16 (N)	1.87 (N)
Lateral Pinch	4.08 (N)	2.18 (N)

The experiments are conducted by a person with spinal cord injury.

Supplementary Material

Supplementary Appendix S1
Supplementary Appendix S2
Supplementary Appendix S3
Supplementary Appendix S4
Supplementary Video S1

References

1. Snoek GJ, Ijzerman MJ, Hermens HJ, et al. Survey of the needs of patients with spinal cord injury: Impact and priority for improvement in hand function in tetraplegics. Spinal Cord 2004;42(9):526–532.
2. Vitrikas K, Dalton H, Breish D. Cerebral palsy: An overview. Am Fam Physician 2020;101(4):213–220.
3. Twitchell TE. The restoration of motor function following hemiplegia in man. Brain 1951;74(4):443–480.
4. Kim DH, Lee Y, Park H-S. Bioinspired High-Degrees of Freedom Soft Robotic Glove for Restoring Versatile and Comfortable Manipulation. Soft Robotics 2021;00(00):1–11.
5. Tran P, Jeong S, Wolf SL, et al. Patient-specific, voice-controlled, robotic flexotendon glove-ii system for spinal cord injury. IEEE Robot Autom Lett 2020;5(2):898–905.
6. Kim DH, Heo SH, Park HS. Biomimetic finger extension mechanism for soft wearable hand rehabilitation devices. IEEE Int Conf Rehabil Robot 2017;2017:1326–1330.
7. Kim B, In H, Lee D-Y, et al. Development and assessment of a hand assist device: GRIPIT. J Neuroeng Rehabil 2017; 14(1):15.
8. Yun Y, Dancausse S, Esmatloo P, et al. "Maestro: An EMG-driven assistive hand exoskeleton for spinal cord injury patients," *Proceedings—IEEE International Conference on Robotics and Automation*, pp. 2904–2910, 2017.
9. Esmatloo P, Deshpande AD. "Fingertip position and force control for dexterous manipulation through model-based control of hand-exoskeleton-environment," *IEEE/ASME International Conference on Advanced Intelligent Mechatronics, AIM*, 994–1001, 2020.

10. Cempini M, Marzegan A, Rabuffetti M, et al. Analysis of relative displacement between the HX wearable robotic exoskeleton and the user's hand. J Neuroeng Rehabil 2014; 11(1):147.
11. Shahid T, Gouwanda D, Nurzaman SG, et al. Moving toward soft robotics: A decade review of the design of hand exoskeletons. Biomimetics 2018;3(3):17.
12. Dragusanu M, Iqbal MZ, Baldi TL, et al. Design, development, and control of a hand/wrist exoskeleton for rehabilitation and training. IEEE Trans Robot 2022;38(3):1472–1488.
13. Li J, Zheng R, Zhang Y, et al. "ihandrehab: An interactive hand exoskeleton for active and passive rehabilitation," in *2011 IEEE International Conference on Rehabilitation Robotics*, pp. 1–6, IEEE, 2011.
14. Vinjamuri R. *Advances in motor neuroprostheses*. Springer, 2020.
15. Lee SW, Landers KA, Park HS. Development of a biomimetic hand exotendon device (BiomHED) for restoration of functional hand movement post-stroke. IEEE Trans Neural Syst Rehabil Eng 2014;22(4):886–898.
16. Kim DH, Park HS. "Cable Actuated Dexterous (CADEX) Glove for Effective Rehabilitation of the Hand for Patients with Neurological diseases," *IEEE International Conference on Intelligent Robots and Systems*, pp. 2305–2310, 2018.
17. In H, Jeong U, Lee H, et al. A Novel Slack-Enabling Tendon Drive That Improves Efficiency, Size, and Safety in Soft Wearable Robots. IEEE/ASME Trans Mechatron 2017; 22(1):59–70.
18. Chen W, Li G, Li N, et al. and "Soft Exoskeleton With Fully Actuated Thumb Movements for Grasping Assistance," *Transactions on Robotics*, pp. 1–14, 2022.
19. Awad LN, Bae J, O'Donnell K, et al. A soft robotic exosuit improves walking in patients after stroke. Sci Transl Med 2017;9(400):eaai9084.
20. Xiloyannis M, Chiaradia D, Frisoli A, et al. Physiological and kinematic effects of a soft exosuit on arm movements. J Neuroeng Rehabil 2019;16(1):29.
21. Choi H, Kang BB, Jung B-K, et al. Exo-wrist: A soft tendon-driven wrist-wearable robot with active anchor for dart-throwing motion in hemiplegic patients. IEEE Robot Autom Lett 2019;4(4):4499–4506.
22. Georgarakis A-M, Xiloyannis M, Wolf P, et al. A textile exomuscle that assists the shoulder during functional movements for everyday life. Nat Mach Intell 2022;4(6): 574–582.
23. Bae J, Siviy C, Rouleau M, et al. "A lightweight and efficient portable soft exosuit for paretic ankle assistance in walking after stroke," in *2018 IEEE international conference on robotics and automation (ICRA)*, pp. 2820–2827, IEEE, 2018.
24. Slade P, Kochenderfer MJ, Delp SL, et al. Personalizing exoskeleton assistance while walking in the real world. Nature 2022;610(7931):277–282.
25. Yang X, Huang T-H, Hu H, et al. Spine-inspired continuum soft exoskeleton for stoop lifting assistance. IEEE Robot Autom Lett 2019;4(4):4547–4554.
26. Ozawa R, Kobayashi H, Hashirii K. Analysis, classification, and design of tendon-driven mechanisms. IEEE Trans Robot 2014;30(2):396–410.
27. Xiloyannis M, Alicea R, Georgarakis A-M, et al. Soft robotic suits: State of the art, core technologies, and open challenges. IEEE Trans Robot 2022;38(3):1343–1362.
28. In H, Kang BB, Sin M, et al. Exo-glove: A wearable robot for the hand with a soft tendon routing system. IEEE Robot Automat Mag 2015;22(1):97–105.
29. Kim B, Ryu J, Cho K-J. Joint Angle Estimation of a Tendon-driven Soft Wearable Robot through a Tension and Stroke Measurement. Sensors (Switzerland 2020;20(10): 2852.
30. Burns MK, Vinjamuri R. *Design of a Soft Glove-Based Robotic Hand Exoskeleton with Embedded Synergies*, pp. 71–87. Springer International Publishing. Cham; 2020.
31. Heung KH, Tang ZQ, Ho L, et al. and "Design of a 3d printed soft robotic hand for stroke rehabilitation and daily activities assistance," in *2019 IEEE 16th international conference on rehabilitation robotics (ICORR)*, pp. 65–70, IEEE, 2019.
32. Ang BW, Yeow C-H. "Print-it-yourself (piy) glove: A fully 3d printed soft robotic hand rehabilitative and assistive exoskeleton for stroke patients," in *2017 IEEE/RSJ International Conference on Intelligent Robots and Systems (IROS)*, pp. 1219–1223, IEEE, 2017.
33. Chen W, Li G, Li N, et al. Soft exoskeleton with fully actuated thumb movements for grasping assistance. IEEE Trans Robot 2022;38(4):2194–2207.
34. Xiloyannis M, Cappello L, Khanh DB, et al. and "Modelling and design of a synergy-based actuator for a tendon-driven soft robotic glove," in *2016 6th IEEE International Conference on Biomedical Robotics and Biomechatronics (BioRob)*, pp. 1213–1219, IEEE, 2016.
35. Alicea R, Xiloyannis M, Chiaradia D, et al. A soft, synergy-based robotic glove for grasping assistance. Wearable Technol 2021;2:e4.
36. Cappello L, Meyer JT, Galloway KC, et al. Assisting hand function after spinal cord injury with a fabric-based soft robotic glove. J Neuroeng Rehabil 2018;15(1):59–10.
37. Kang BB, Choi H, Lee H, et al. Exo-Glove Poly II: A Polymer-Based Soft Wearable Robot for the Hand with a Tendon-Driven Actuation System. Soft Robot 2019;6(2): 214–227.
38. Soucacos PN. Indications and selection for digital amputation and replantation. J Hand Surg Br 2001;26(6): 572–581.
39. Kim B, Jeong U, Kang BB, et al. Slider-Tendon Linear Actuator with Under-actuation and Fast-connection for Soft Wearable Robots. IEEE/ASME Trans Mechatron 2021; 26(6):2932–2943.
40. Chang LY, Srinivasa SS, Pollard NS. and "Planning pre-grasp manipulation for transport tasks," *Proceedings—IEEE International Conference on Robotics and Automation*, pp. 2697–2704, 2010.
41. Eppner C, Brock O. "Planning grasp strategies That Exploit Environmental Constraints," *Proceedings—IEEE International Conference on Robotics and Automation*, pp. 4947–4952, 2015.
42. Lee DH, Park JH, Park SW, et al. KITECH-Hand: A Highly Dexterous and Modularized Robotic Hand. IEEE/ASME Trans Mechatron 2017;22(2):876–887.
43. Chen Y, Le S, Tan QC, et al. and "A lobster-inspired robotic glove for hand rehabilitation," *Proceedings—IEEE*

International Conference on Robotics and Automation, pp. 4782–4787, 2017.

44. Rose CG, O'Malley MK. Hybrid Rigid-Soft Hand Exoskeleton to Assist Functional Dexterity. IEEE Robot Autom Lett 2019;4(1):73–80.
45. Heung KH, Tong RK, Lau AT, et al. Robotic glove with soft-elastic composite actuators for assisting activities of daily living. Soft Robot 2019;6(2):289–304.
46. Villoslada A, Rivera C, Escudero N, et al. Hand exomuscular system for assisting astronauts during extravehicular activities. Soft Robot 2019;6(1):21–37.
47. Zhang T, Huang H. A lower-back robotic exoskeleton: Industrial handling augmentation used to provide spinal support. IEEE Robot Automat Mag 2018;25(2): 95–106.
48. Agarwal P, Deshpande AD. Subject-specific assist-as-needed controllers for a hand exoskeleton for rehabilitation. IEEE Robot Autom Lett 2018;3(1):508–515.

Address correspondence to:
Kyu-Jin Cho
Biorobotics Laboratory
Department of Mechanical Engineering/Soft Robotics Research Center (SRRC)/Institute of Advanced Machines and Design (IAMD)/Institute of Engineering Research
Seoul National University
Seoul
Korea

E-mail: kjcho@snu.ac.kr